Article

Not peer-reviewed version

Encapsulation of Recombinant ACE-2 in Chitosan Nanoparticles for Treatment of SARS-CoV-2 Infection

Yigong Guo , Alberto Baldelli , Dai Shi , David D Kitts , Anubuav Pratap-Singh , Anika Singh *

Posted Date: 8 February 2025

doi: 10.20944/preprints202502.0602.v1

Keywords: Covid-19; ACE-2; Nanoparticles; Spray Freeze Dry (SFD)

 doi:10.20944/preprints202502.0602.v1

Article

Encapsulation of Recombinant ACE-2 in Chitosan Nanoparticles for Treatment of SARS-CoV-2 Infection

Yigong Guo [1], Alberto Baldelli [2], Dai Shi [2], David D. Kitts [2], Anubhav Pratap-Singh [2] and Anika Singh [1,2,*]

[1] Natural Health and Food Products Research Group, Centre for Applied Research and Innovation (CARI), British Columbia Institute of Technology, 4355 Mathissi Pl, Burnaby, BC, V5G 4S8, Canada

[2] Food, Nutrition, and Health, Faculty of Land & Food Systems. 2205 East Mall, University of British Columbia, Vancouver, BC, Canada, V6T 1Z4

* Correspondence: anika_singh@bcit.ca; Tel.: +604-723-9545

Abstract: COVID-19 infection continues globally with frequent emergence of unfamiliar SARS-CoV-2 variants acting to impair immunity conferred by vaccines. The competitive binding of SARS-CoV-2 spike proteins by angiotensin-converting enzyme 2 (ACE-2) to mimetic and act as a decoy over that by native ACE-2 receptors on healthy human cells remains a practical approach to lessen viral spread. In this study, a therapeutic strategy was developed that targeted gastrointestinal SARS-CoV-2 infection using ACE-2 encapsulated in chitosan/tripolyphosphate cross-linked nanoparticles (NPs). Optimization conditions were determined by varying pH (4.0-6.5) and chitosan: ACE-2 mixing ratios (1:1, 1.5:1, 2:1, 2.5:1, 3:1), followed by choice of spray-drying (SD), freeze-drying (FD), or spray-freeze drying (SFD) with varying mannitol concentrations (0, 1:1, and 5:1 of total weight). The optimal formulation was achieved using a pH 5.5 with a mixing chitosan-ACE-2 ratio of 2:1; where ACE-2 loaded NPs had an average particle size of 303.7 nm, polydispersity index (PDI) of 0.21, encapsulation efficiency (EE) of 98.4%, zeta potential of 6.8 mV, and ACE-2 loading content (LC) of 28.4%. In general, all drying methods maintained the spherical shape of the NPs with varying mannitol concentration having a significant ($P<0.05$) effect. After reconstitution, all SD samples had a relatively low yield rate, but the ACE-2 NPs dehydrated specifically by SFD required a lower amount of added mannitol (1:1 of its total weight) and produced a higher yield rate ($P<0.05$) and similar PDI and EE values, along with relatively good particle size and LC. This formulation also produced a high ACE-2 release and uptake in differentiated Caco-2 cells; thus, representing an effective ACE-2 encapsulation procedure for use with dry powders.

Keywords: COVID-19; ACE-2; nanoparticles; spray freeze dry (SFD)

1. Introduction

Although COVID-19 cases are now lower than the pandemic stage, this contagious disease continues to affect global populations with varying transmission rates and severity across regions (WHO, 2024). The ongoing emergence of SARS-CoV-2 variants renders existing vaccines less effective, underlining the pressing need for new therapeutic strategies needed to control this disease [1]. SARS-CoV-2 invades the human body through the binding interaction between the surface spike proteins and the angiotensin-converting enzyme 2 (ACE-2) receptors present on healthy human cells, involved with triggering virus-cell fusion and the release of viral genetic materials for replication [2,3]. As mutated SARS-CoV-2 tends to retain a high binding affinity to the ACE-2 receptors, therapeutic approaches that block or reduce the occurrence of such interactions remain practical approaches to lessen COVID-19 infection [1,4]. Although effective in reducing viral spread, the primary intravenous administration route of ACE-2 derivatives requires frequent supplementation

 doi:10.20944/preprints202502.0602.v1

to maintain a sufficient drug concentration, due to a rapid degradation in free forms [1,5]. Intravascular delivery also exhibits low transportation rates across plasma-lung barriers and is considered as an inconvenient delivery route, further limiting its therapeutic efficacy [1].

To find a solution to enhance the effectiveness of exogenous ACE-2, nanocarrier systems have been explored for a protective role to aid absorption-enhancing capacity of embedded drugs. It can be garnered that the majority of ACE-2 nanocarrier studies indeed target application to respiratory epithelial cells, logically given that COVID-19 is a primarily respiratory illness. However, as pointed out by Sajdel-Sulkowska, (2021), since the levels of ACE-2 receptors distributed in the gastrointestinal (GI) tract far exceed those in the respiratory tract, the oral route of infection could be reason to establish a viable approach with designed novel ACE-2 based therapeutic approaches. Moreover, to minimize SARS-CoV-2 spread within the human body more comprehensively, GI delivery of exogenous ACE-2 warrants more in-depth investigation.

Chitosan, being the sole naturally occurring cationic polysaccharide (pKa of ~6.5), is highly mucoadhesive to negatively charged surfaces such as those in the GI tract, thus prolonging the contact with target tissues and enhancing drug delivery as an encapsulation matrix [6,7]. These electrostatic interactions also enhance the permeability of biological membranes by opening the epithelial tight junctions of to improve absorption of poorly permeable compounds via both the paracellular and transcellular transportation routes [7]. The preparation of chitosan-based NPs typically includes emulsification, precipitation, and ionic gelation methods, the last of which is advantageous as it is simple and a mild procedure without the application of organic solvents or high temperatures [8]. Cationic chitosan when suspended in aqueous solutions readily complexes with anionic agents, a popular one of which is tripolyphosphate (TPP). Nanoparticles generated from chitosan/TPP mixtures generally have uniform particle size, low cellular toxicity and high encapsulation efficiency and loading capacity [9]. This technique has been extensively used to encapsulate natural bioactives, synthetic drugs, and therapeutic proteins and peptides [9]. To date, there has been no report on the encapsulation of ACE-2 using chitosan/TPP NPs.

Ingredient dehydration (e.g., powder production) is a common practice in the food and pharmaceutical industry to preserve the desirable characteristics of products while also extending shelf-life, thus saving on packaging, transportation, and storage costs. Likewise, freshly prepared NPs are typically dehydrated into dry powder forms before they are ready to use directly or added into other formulations. Spray-drying (SD) is the most applied dehydration technique for this purpose as it is an economic, quick, and a continuous process [10,11]. The technique involves the atomization (spraying) of a feed solution into a drying chamber where hot air is circulated. Due to the high temperatures required to immediately evaporate water, thermal damage can occur especially on heat-sensitive compounds (e.g., proteins). A popular alternative to avoid ingredient thermal degradation is to use freeze-drying (FD), where mass (water) transfer is carried out by sublimation of ice crystals within the frozen feed. However, due to the long processing time (2.5 times higher than SD) and the high energy input, required to deliver lower-pressure environments, the production is relatively expensive [10,12]. To overcome the limitations arising from both SD and FD, a combinative approach termed 'spray-freeze drying' (SFD) has been developed. Similarly in SD, the feed solution is first atomized into fine droplets directly into a cryogenic zone filled with liquid nitrogen; here the frozen droplets are collected for subsequent drying following the typical FD protocol. By reducing product dimensions through spraying, mass transfer in the freeze dryer is significantly enhanced, hence an overall shorter process with lower costs is realized [12]. The quick freezing involved in SFD also allows particles to retain a spherical shape while achieving a large, highly porous specific surface area, drastically improving reconstitution ability [13] and drug release [14].

The overarching goal of the present research was to produce encapsulated ACE-2 via chitosan/TPP NP matrix and to evaluate stability, bioactivity and drug release functionality. Formulation variables were tested by varying pH (4.0-6.5) and chitosan: ACE-2 mixing ratios (1:1, 1.5:1, 2:1, 2.5:1, 3:1) in order to optimize particle size, drug loading and entrapment efficiency. In

 doi:10.20944/preprints202502.0602.v1

addition, freshly prepared NPs were dehydrated employing three different methods, including SD, FD, and SFD at different (0, 1:1, and 5:1) mannitol concentrations for optimal NP morphological properties, yield rate, reconstitution (rehydration), stability, and *in vitro* release, cellular uptake, and toxicity assessment in cultured Caco-2 cells.

2. Materials and Methods

2.1. Materials

The ACE-2 used in this study was kindly provided by Dr. David Perrin, UBC Chemistry (Vancouver, BC, Canada). Low MW chitosan (average MW 100 KDa, 75-85% deacetylated), TPP, and essential cell culture medium were purchased from Sigma-Aldrich (Oakville, ON, Canada). All other reagents used were of analytical grade or HPLC grade. Caco-2 cells (HTB-37, American Type Culture Collection, Manassas, VA, USA) were cultured in Dulbecco's Modified Eagle Medium (DMEM) media (Invitrogen, Carlsbad, ON, Canada) and supplemented with 10% fetal bovine serum (FBS) and 100 U/mL of penicillin and streptomycin, respectively (Sigma, St. Louis, MO, USA).

2.2. ACE-2 Nanoparticles Preparation

The ACE-2 NPs were prepared using an ion-gelation method. Briefly, the ACE-2 was first mixed with TPP solution to which a chitosan solution was added dropwise under high-speed stirring (10,000 rpm) using a polytron PCU-2-110 high-speed homogenizer (Brinkmann Ind., Westbury, NY, USA). After adjusting the pH, the mixed solution was maintained under high-speed stirring (15,000 rpm) in an ice bath for another 30 min to obtain crosslinked ACE-2 NPs. Sonication was used to process samples for an additional 30 min in an ice bath using a probe-type ultrasonicator (UP 200ST, Hielscher Ultrasonics, Teltow, Germany) to reduce the particle size of ACE-2 NPs. The ACE-2 NPs were prepared at six different pHs (4- 6.5) with varying ratios (1:1, 1.5:1, 2:1, 2.5:1, 3:1) between chitosan and ACE-2 to obtain optimized NPs.

2.3. Dehydration of the ACE-2 NPs

Three dehydration techniques were used to prepare ACE-2 NP dry powder, using freeze-drying (FD), spray-drying (SD), and spray-freeze drying (SFD), respectively. Mannitol was added to each sample at ratios of 0, 1:1, and 5:1 of total NP weight. A Labconco FreeZone freeze-dryer equipped with tray dryers (Labconco, Kansas City, MO, USA) was used to prepare FD ACE-2 NPs. The temperature and vacuum pressure were set at -10 °C and 0.350 Torr, respectively, for the first 2 h, and at 0 °C and 0.120 Torr, respectively, for the remaining 22 h to obtain dry ACE-2 NPs. For SD, a Buchi mini spray dryer B-290 (BÜCHI, Flawil, Switzerland) was used. The drying parameters selected were inlet temperature of 90 °C, outlet temperature of 40 °C, a feeding flow rate of 6 mL/min, and an airflow rate of 4 L/min. For SFD, the drying chamber of the spray dryer was replaced with a laboratory jacket containing a cylindrical borosilicate glass Dewar flask (250 mL, StonyLab, Nesconset, NY, USA) filled with liquid nitrogen. The distance between the atomizer and the surface of the liquid nitrogen was set at 10 cm. The ACE-2 NPs were directly sprayed into the liquid nitrogen at a feeding flow rate of 5 mL/min and an airflow rate of 4 L/min. After that, the frozen ACE-2 NPs were further dehydrated using a freeze dryer and the same set of parameters mentioned above were used.

2.4. Characterization of Nanoparticles

The mean diameter, polydispersity index (PDI), and zeta potential of ACE-2 NPs were determined by dynamic light scattering (DLS) using a Litesizer 500 (Anton Paar, Graz, Austria). A scanning electron microscope (SEM) (Hitachi S4700 SEM, field emission gun ultra-high-resolution SEM) was used to measure the morphology of dehydrated ACE-2 NPs. To evaluate the encapsulation efficiency (EE) of ACE-2 NPs, ultrafiltration tubes with a MW cutoff of 100 kDa were used, and ACE-

 doi:10.20944/preprints202502.0602.v1

2 NPs were added and centrifuged at 500 × g for 30 min. The free ACE-2 present in the filtrate was quantified using an Agilent 1100 series HPLC system (Agilent, Santa Clara, CA, USA) with a quaternary pump, an autosampler, a column heater, and a diode array detector. ACE-2 was quantifed from a C18 column (Zorbax, 3.5 µm, 4.6 mm × 150 mm, Agilent, Santa Clara, CA, USA) and detected at 220 nm. The mobile phase consisted of acetonitrile and water with 0.1% trifluoroacetic acid, running at a gradient ratio of 10:90 to 100:0 for 10 min. The EE of the ACE-2 NPs in percentages were calculated using Eq. (1). The loading content (LC) of the ACE-2 NPs was calculated as the ratio between the total weight of loaded ACE-2 and the total weight of ACE-2 NPs, as shown in Eq. (2)

$$EE\ (\%) = \left(1 - {free\ ACE-2}/{Total\ ACE-2}\right) \times 100\% \quad (1)$$

$$LC\ (\%) = \left({Weight\ of\ loaded\ ACE-2}/{Weight\ of\ NPs}\right) \times 100\% \quad (2)$$

2.5. Fourier Transform Infrared-Attenuated Total Reflectance (FTIR-ATR) Spectroscopy

Free ACE-2, chitosan, freshly prepared ACE-2 NPs, and ACE-2 NPs dehydrated with different methods were characterized by FTIR-ATR spectroscopy using a Spectrum 100 FTIR spectrophotometer equipped with universal ATR sampling accessories (PerkinElmer, Waltham, MA, USA). Signal averages were obtained from 16 scans in the frequency range of 4000-600 cm^{-1} at a resolution of 4 cm^{-1}.

2.6. Reconstitution Test

All dehydrated ACE-2 NPs were redissolved in double distilled water to conduct a reconstitution test. The particle size, PDI, EE, and LC were retested using the same method as previously described to evaluate quality after reconstitution. The yield of the ACE-2 was also calculated based on the ratio between the ACE-2 before and after reconstitution.

2.7. In Vitro Release Profile of ACE-2 Loaded NPs

The *in vitro* release behaviour of freshly prepared and dehydrated ACE-2 NPs was tested using a dialysis bag method (MW cutoff of 100 kDa, Spectra Por Inc., Rancho Dominguez, CA, USA). Freshly prepared and redissolved dried ACE-2 NPs were dialyzed into pH 2.5, 6.0, and 7.0 (0.1 M phosphate-buffered saline, PBS) model solutions with pepsin, thereby representing the pH environment of the stomach, duodenum, and upper small intestine, respectively. All samples were incubated at 37 °C with continuous shaking at 200 rpm, and 5 mL of the liquid outside the dialysis bag was withdrawn at the following time points: 0.5, 1, 2, 3, 4, and 6 h. The volume was immediately replenished with fresh dialysis model solution. The content of the ACE-2 was measured by HPLC, and the rate of ACE-2 release from the NPs was calculated as the ratio between released free ACE-2 and the total amount of ACE-2 encapsulated in the NPs.

2.8. In Vitro Cellular Uptake Study

Free ACE-2 and ACE-2 NPs dehydrated by different methods were tested for cellar uptake using a cell lysis method that included Caco-2 cells seeded at a density of 5 × 10^4 cells/cm^2 in a 24-well plate and cultivated for 21 days to establish differentiation before testing. Cells were treated with free ACE-2 and ACE-2 NPs dehydrated by different methods, respectively, for 6 h, and then extracted by lysis buffer to release intracellular ACE-2 for subsequent analysis using HPLC with pure ACE-2 standard.

2.9. In Vitro Cytotoxicity Assay

The MTT test was used to assess the cytotoxicity of dehydrated ACE-2 NPs at varying concentrations. Differentiated Caco-2 cells were seeded at a density of 5 × 10^4 cells/cm^2 in 96-well plates. Free ACE-2 and ACE-2 NPs dehydrated by different methods were diluted in concentrations

 doi:10.20944/preprints202502.0602.v1

ranging from 50 to 500 μg/mL in culture medium and then applied to the cells. After a 24-h incubation, the cells were washed and refreshed with a medium containing 0.5 mg/mL of MTT followed by another 2 h of incubation. Cytotoxicity was measured by recording the enzymatic reduction of yellow tetrazolium MTT to purple formazan at 550 nm using a Tecan Infinite M200 Pro spectrophotometer plate reader (Tecan, Mennedorf, Switzerland).

2.10. Statistical Analysis

All experiments were performed in triplicate (n=3). The values are presented as mean ± standard deviation. All data were evaluated using a one-way ANOVA or a paired t-test by IBM SPSS Statistics 26 (IBM, Endicott, NY, USA).

3. Results and Discussion

3.1. Optimization of Chitosan-TPP Cross-Linked ACE-2 NPs

It was critical to control the pH of the mixing solution and the ratio between ACE-2 and chitosan because they had direct impacts on the formation of the NPs by influencing the final particle size and EE. Particle size exhibited a high association with the pH of the mixing solution (Figure 1A). The mean particle size (nm) of ACE-2 loaded NPs was reduced, and the EE was increased, when the pH of the system increased from 4.0 to 5.5, while the mean particle size started to increase, and the EE remained the same, once the pH further increased to 6.5 (Figure 1A,C). Besides, as the ratio of chitosan to ACE-2 increased, the mean particle size also tended to increase (Figure 1B). Chitosan is a weak polyelectrolyte with a pKa value of ~6.5. In acidic media, the presence of a predominant amino group is protonated by hydrogen ions thus exhibiting a positive charge. Therefore, this condition is often used as a carrier to encapsulate negatively charged molecules. In this study, chitosan was used to encapsulate ACE-2 with an isoelectric point of 5.4. [15] investigated the effect of pH on the particle size of chitosan NPs. They found that there was a continuous decrease in particle size before pH reached a value around 5.5, and a significant increase in size was observed at pH >5.5. This is consistent with our observations (Figure 1A). This phenomenon was due to the ACE-2 molecules acquiring a negative surface charge as the pH increased, which facilitated electrostatic interactions with the chitosan/TPP complex and resulting in a decrease in particle size and an increase in EE. However, adjusting the pH to 6.5 led to the deprotonation of the amino groups on chitosan, causing it to fold. Thus, higher pH exposed fewer amino ions to TPP and ACE-2, resulting in less cross-linking and ultimately larger particle size and lower EE. Furthermore, the higher the chitosan content, the more ACE-2 can be encapsulated. Since chitosan acted as a coating material, increasing its proportion would correspondingly increase the thickness of the outer layer of the NPs, resulting in a larger particle size and higher EE. In this case, the highest EE was reached when the chitosan to ACE-2 ratio reached 2:1, and no significant change in EE was observed with further increase in the ratio (Figure 1D). Therefore, the optimal preparation condition obtained in this study was at pH 5.5 and ACE-2/chitosan mass ratio of 2:1 to prepare ACE-2-loaded NPs for further studies. Under this preparation condition, ACE-2 NPs had an average particle size of 303.7 nm, PDI of 0.21, EE of 98.4%, zeta potential of 6.8 mV, and ACE-2 LC of 28.4% (Figure S1).

 doi:10.20944/preprints202502.0602.v1

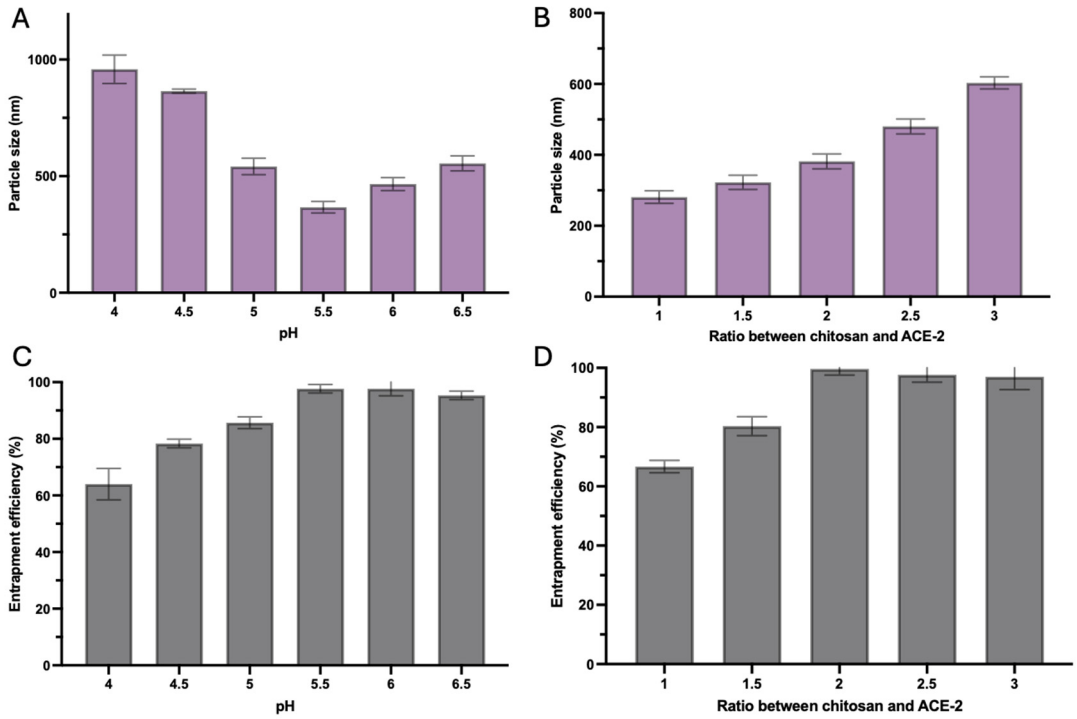

Figure 1. Optimization of parameters for ACE-2 NPs: A) Effect of pH on particle size (prepared at the 3:1 mass ratio of chitosan and ACE-2); B) Effect of mass ratio between chitosan and ACE-2 on particle size (prepared at pH 6); C) Effect of pH on entrapment (encapsulation) efficiency (prepared at the 3:1 mass ratio of chitosan and ACE-2); and D) Effect of mass ratio between chitosan and ACE-2 on entrapment (encapsulation) efficiency (prepared at pH 6). Values represent means ± SD (n=3).

3.2. Morphological Analysis of ACE-2 NPs Dehydrated by Different Methods

The analysis of the morphological characteristics of FD, SD, and SFD ACE-2 NPs were performed to to select more appropriate dehydration techniques for powder formation. The preferred approach should provide drug stability, uniform particle shape, high drug loading, and good reconstitution ability. In this study, as FD techniques were involved, the impact of mannitol as a bulking agent was also evaluated. In all three dehydration techniques, mannitol played a dual role as a filler and a cryoprotector. ACE-2 NPs without mannitol, with mannitol of its total weight of 1:1 and 5:1 was tested in this study. For FD ACE-2 NPs without mannitol, a highly porous structure with irregular and rough surface was observed by SEM, as shown in Figure 2. After dehydration, only few particles could be detected in the mixture. This result indicated that most of the ACE-2 NPs were degraded during the process of FD without mannitol present as a cryoprotectant. With the assistance of mannitol, a portion of the spherical particles can be detected in FD ACE-2 NPs with mannitol present at weight ratio of 1:1. For SD ACE-2 NPs with mannitol present had weight ratios of 1:1 and 5:1, SFD with mannitol of its total weight of 1:1 and 5:1, and FD with mannitol present had total weight ratio of 5:1; with spherical particles and a smooth surface observed. Besides, SD ACE-2 NPs without mannitol present retained the spherical structure, but with craggy surfaces, while SFD ACE-2 NPs without mannitol present resulted in a spherical structure with highly porous surfaces.

During FD, mannitol acted as a cryoprotectant and remained in an amorphous form, protecting the ACE-2 NPs from damage caused by ice crystals. In contrast, the SD process without a freezing step could promote encapsulation during the dehydration process. Therefore, mannitol was not always required for the SD process, but it could still serve as a bulking agent to give the ACE-2 NPs a more spherical structure. This is seen with SD ACE-2 NPs without mannitol, where particles maintained a spherical structure, but with craggy surfaces (Figure 2). Furthermore, it was revealed that some large particles were detected in all FD, SD, and SFD ACE-2 NPs products, containing high amount of mannitol. This was likely due to the accumulation of mannitol in the particle core together

 doi:10.20944/preprints202502.0602.v1

with ACE-2 within the chitosan capsule layer. Noticeably, it can be seen that using SFD also protected the spherical structure of the ACE-2 NPs. This can be attributed to the quick-free of the ACE-2 NPS and part of the water from the first spraying step of SFD using liquid nitrogen going transferring to fine ice crystal rather than formation of undesirable irregular large ice crystals. Thus, even in the absence of mannitol the spherical structure and quality of pores on the surface of ACE-2 NPs were acceptable. This was further enhanced with low mannitol (1:1 of mannitol to the total weight of ACE-2 NPs) present and required for employing the SFD technique in ordr to obtain ACE-2 NPs powders with intact surfaces and smaller particles.

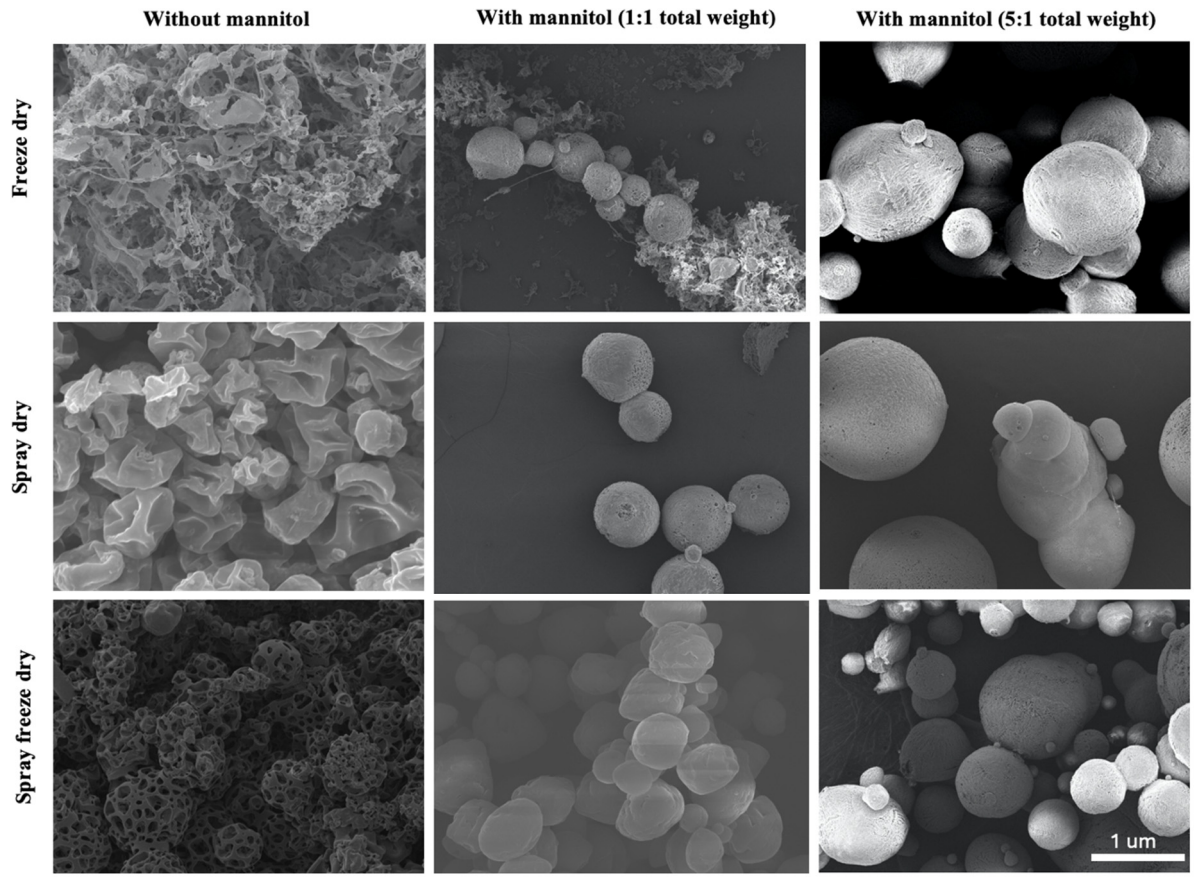

Figure 2. Morphology (SEM) of ACE-2 NPs dehydrated by different methods.

3.3. FTIR-ATR Spectroscopy Analysis

The FTIR-ATR spectroscopy characterized free ACE-2, chitosan, a physical mixture of chitosan, TPP, and ACE-2, and ACE-2 loaded NPs that were dehydrated using different methods. Particularly, band intensities appearing at 1639, 1548, and 1408 cm^{-1} were observed for SD and SFD dehydrated ACE-2 NPs at all mannitol concentrations tested, and also with FD using a mannitol total weight ratio of 5:1 (Figure 3). The observed increases in matrix strength are attributed to the cross-linking between chitosan, TPP and ACE-2 [16], The chitosan-ACE-2 interaction showed in FTIR-ATR spectra reflect the overlapping of the chitosan bands with those of ACE-2, resulting in an increase in the carbonyl intensity band (1639 cm^{-1}) and amine band (1548 cm^{-1}), respectively. The TPP tripolyphosphate group had attached to the ammonium group of chitosan to give rise of a band at 1412 cm^{-1}. Furthermore, these results were consistent with those SEM spectra (Figure 2), where ACE-2 NPs remained intact upon SD and SFD at all mannitol concentrations, along with FD samples that had mannitol total weight of 5:1. In contrast, NPs without mannitol or having the lowest mannitol ratio (e.g., 1:1) gave FTIR-ATR spectra that were very similar to the physical mixture of chitosan, TPP, and ACE-2. From this, we conclude that the cross-linking between chitosan, TPP, and ACE-2 was no longer present in FD ACE-2 NPs in the absence of mannitol, or also present at very low ratios. This was confirmed with

 doi:10.20944/preprints202502.0602.v1

the SEM findings shown in (Figure 2). Since only FD ACE-2 NPs were especially fragile and broke during FD dehydration they were not used for subsequent *in vitro* tests.

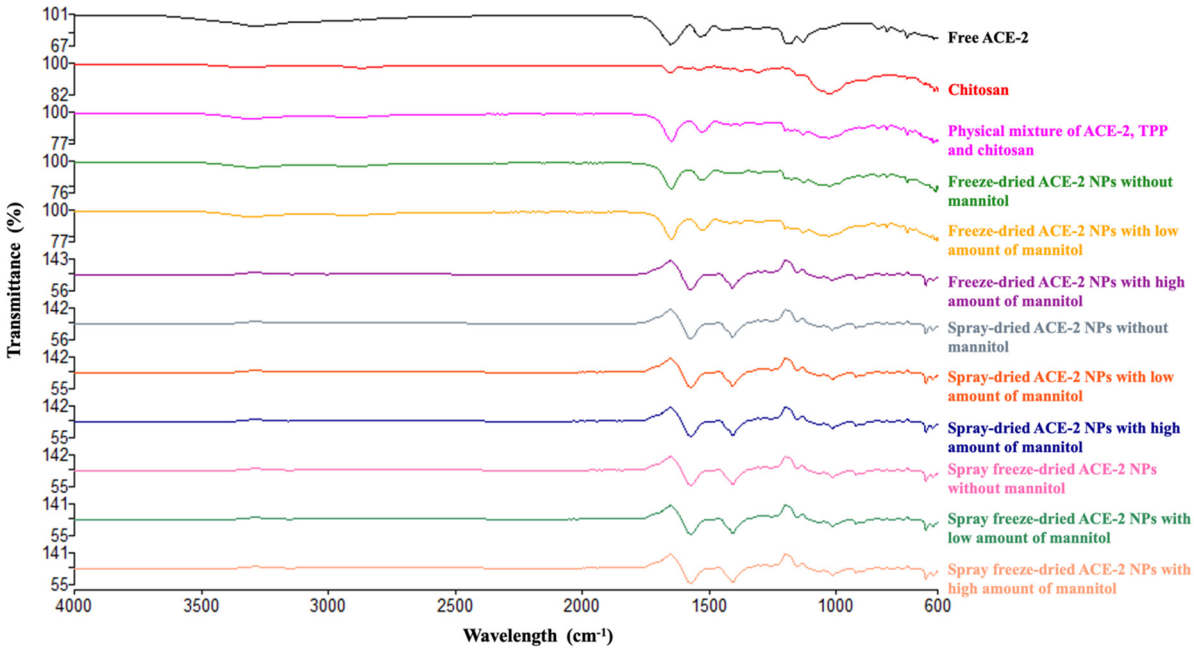

Figure 3. FTIR-ATR spectra of free ACE-2, chitosan, physical mixture of chitosan/TPP/ACE-2 and ACE-2 NPs dehydrated at varying mannitol concentrations by different drying methods. The different conditions used to derive the NPs are given at the right of the diagram spectrum.

3.4. Yield Rate, Reconstitution and Stability Analysis

Dehydrated NPs are typically used for long-term storage or reprocessing into other formulations, and thus the capacity of dried NPs to reconstitute into water is important for successful use in various formulations. In this study, results indicated that the yield rate and LC of all SD samples were lower than those treated with FD and SFD (Table 1) (Figure S2). This outcome can be attributed by the adhesion of powder particles to the drying chamber wall. Since ACE-2 is temperature sensitive, having the presence of mannitol and using a relatively low outlet temperature (40 °C) reduced to some extent ACE-2 degradation during the SD process. It was also found that the average particle size of ACE-2 NPs prepared by SD and SFD without presence of mannitol was preserved after reconstitution. The size of ACE-2 NPs processed by SD and SFD that had small amounts of mannitol (1:1 of its total weight) present were only increased slightly after reconstitution. Increasing the amount of mannitol to its maximum ratio (e.g., 5:1) had a significant effect ($P<0.05$) on the size of ACE-2 NPs prepared by dehydration methods SD, FD, and SFD, respectively. The use of FD processing of ACE-2 NPs produced the largest particle sizes upon reconstitution compared to other drying methods. These results indicate that the use of the bulking agent, mannitol, and control of formation of ice crystals before dehydration were important to increase the particle size of the NPs after reconstitution. In this study, the PDI did not change significantly after reconstitution for all NPs. However, for the EE parameter after reconstitution, the ACE-2 NPs dehydrated by SFD in absence of mannitol was largely reduced, signifying that although the spherical structure of the ACE-2 NPs was not changed the porous surfaces could result in NP leakage of the ACE-2. Furthermore, the addition of mannitol significantly reduced the ACE-2 loading in all NPs tested. It is known that the LC of NPs is an important parameter when assessing use for pharmaceutical applications. For NPs with low LC, very large amounts of NPs are required to reach a therapeutic threshold. Considering all parameters tested in this study, the use of SFD to dehydrate ACE-2 NPs with a low mannitol (1:1 of its total weight) present, was the best set of process conditions used for reconstitution of ACE-NP.

 doi:10.20944/preprints202502.0602.v1

Moreover, these conditions also gave a high yield rate, PDI and EE, respectively, while also maintaining good particle sizes and ACE-2 LC.

Table 1. Physicochemical properties of freshly prepared and reconstituted ACE-2 NPs (one-way ANOVA comparisons, $p<0.05$).

	Freshly prepared	FD ++	SD -	SD +	SD ++	SFD -	SFD +	SFD -
PS (nm)	303 ± 12^{a}	674 ± 47^{b}	343 ± 33^{c}	535 ± 24^{d}	613 ± 37^{b}	366 ± 29^{c}	548 ± 30^{d}	664 ± 42^{b}
PDI	0.19 ± 0.02^{a}	0.24 ± 0.03^{a}	0.22 ± 0.02^{a}	0.23 ± 0.03^{a}	0.25 ± 0.05^{a}	0.22 ± 0.04^{a}	0.21 ± 0.03^{a}	0.20 ± 0.04^{a}
EE (%)	98.40± 0.32^{a}	98.01 ± 0.43^{a}	97.63 ± 0.29^{a}	99.01 ± 0.51^{a}	98.23 ± 0.43^{a}	99.03 ± 0.39^{a}	98.93 ± 0.36^{a}	99.02 ± 0.22^{a}
LC (%)	28.42 ± 0.21^{a}	4.71 ± 0.13^{b}	18.14 ± 0.44^{c}	3.92 ± 0.10^{d}	2.02 ± 0.06^{e}	27.84 ± 0.30^{a}	14.22 ± 0.32^{f}	4.69 ± 0.36^{b}
YR (%)	NA	99.83 ± 0.13^{a}	47.87 ± 2.13^{b}	53.32 ± 3.13^{c}	55.31 ± 2.13^{c}	99.67 ± 0.13^{a}	98.98 ± 0.13^{a}	99.32 ± 0.13^{a}

Abbreviations: FD, freeze-drying; SD, spray-drying; SFD, spray-freeze-drying; PS, particle size; PDI, polydispersity index; EE, encapsulation efficiency; LC, loading content; YR, yield rate; and NA, not applicable. -= no mannitol; + =low mannitol; ++= high mannitol. Values represent mean ± SD (n=3). Differernt superscripts ^{a,b,c,} in rows represent statistical difference (ANOVA; $P<0.05$).

3.5. In Vitro Release of ACE-2 from NPs at Different pHs

To simulate the pH environment of the stomach, duodenum, and upper small intestine, respectively, free ACE-2 and redissolved dried ACE-2 NPs were incubated in different buffers (e.g., pH 2.5, 6.0, 7.0, respectively) with added pepsin (0.5 mg/ml) and incubated at 37 °C in a water bath for 6 hours. All NPs exhibited an initial release of ACE-2 in the first hour, followed by a slow release over the next 5 h in all buffer solutions that simulated different gastrointestinal environments (Figure 4). This observed rapid initial release was attributed to the high concentration difference at the beginning of the incubation period and the rapid surface desorption of ACE-2 molecules that were not completely anchored to the internal structure of the particles. All NPs exhibited the highest release of ACE-2 at pH 7; followed by pH 2.5 and pH 6.0. This result can be attributed to the fact that the deprotonation of chitosan occurs at higher pHs, thus resulting in a less compact polymer network and greater the release of the loaded ACE-2. Furthermore, the SD processed ACE-2 NPs, without mannitol added showed the fastest release profile followed by ACE-2 NPs processed by SD and SFD, respectively, both containing the low amount of mannitol (1:1 of its total weight). Release was different between ACE-2 NPs prepared by SD and SFD, each having a high amount of mannitol (5:1 of its total weight) present, and the FD ACE-2 NPs, also with high amount of mannitol (5:1 of its total weight). This finding is consistent with the relative order of the particle sizes for redissolved ACE-2 NPs (Table 1), where the smallest particle size gave the fastest release rate. Small particles with a larger surface area facilitate the ACE-2 location close to the particle surface, thus resulting in a rapid rate of release. It can also be noticed that SFD processed ACE-2 NPs, without mannitol present, produced relative low ACE-2 release compared with other treatments, indicating that a highly porous surface and the low EE did not protect ACE-2 degradation when in the presence of pepsin.

 doi:10.20944/preprints202502.0602.v1

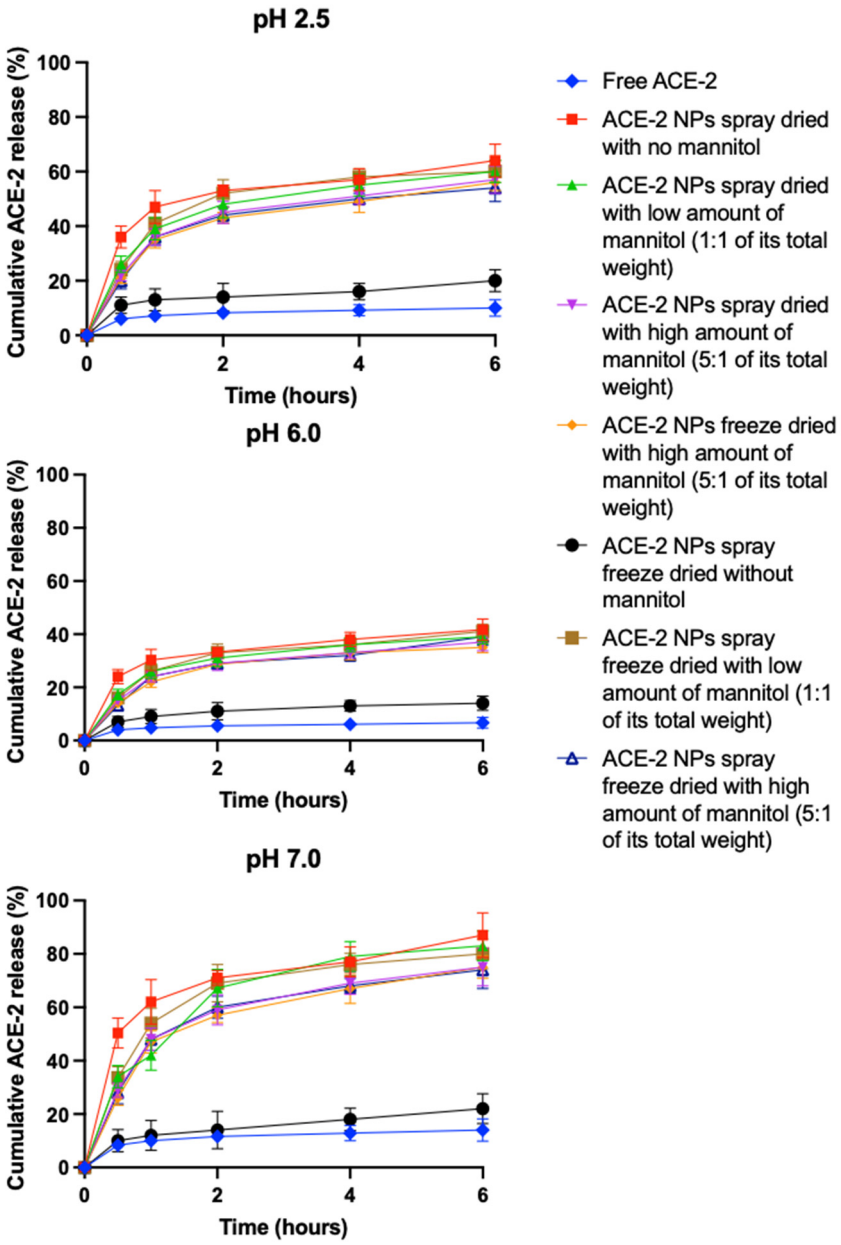

Figure 4. Release behaviors of free ACE-2 and dehydrated ACE-2 NPs at different pHs. Values represent Mean ±SD, N=3.

3.6. In Vitro Cellular (Cacp-2) Uptake of Dehydrated ACE-2 NPs

Free ACE-2 (25µg/mL) along with an equivalent amount of ACE-2 content recovered from freshly prepared ACE-2 NPs, and dry processed ACE-2 NPs were assessed for relative intracellular uptake in Caco-2 cells by cell lysis (Figure 5). The results showed that the SD ACE-2 NPs without mannitol had the highest cellular uptake in differentiated Caco-2 cells, followed by ACE-2 NPs that were dried using SD and SFD, respectively, with low mannitol (1:1 of its total weight). ACE-2 NPs that had high mannitol content (5:1 of its total weight), and SFD dried product had relatively lower uptake ($P<0.05$), as was the case with FD ACE-2 NPs that were prepared using high mannitol (5:1 of its total weight). In addition to having smaller ACE-2 NP showing higher cellular uptake, it was also observed that the addition of mannitol at high concentrations lowered cellular uptake, a feature that was likely due to the increased viscosity of the solution that lowers cellular permeability. It was also observed that although SFD ACE-2 NPs without mannitol having a small particle size and a porous surface was also restricted in retention of the ACE-2 NP after being redissolved. Based on the results above, it is noteworthy that despite the fact that SD ACE-2 NPs with low mannitol exhibited highest

 doi:10.20944/preprints202502.0602.v1

Caco-2 cell uptake, the SFD ACE-2 with low amount of mannitol (1:1 of its total weight) was the preferred process for producing ACE-2 NPs because of a relatively high cellular uptake.

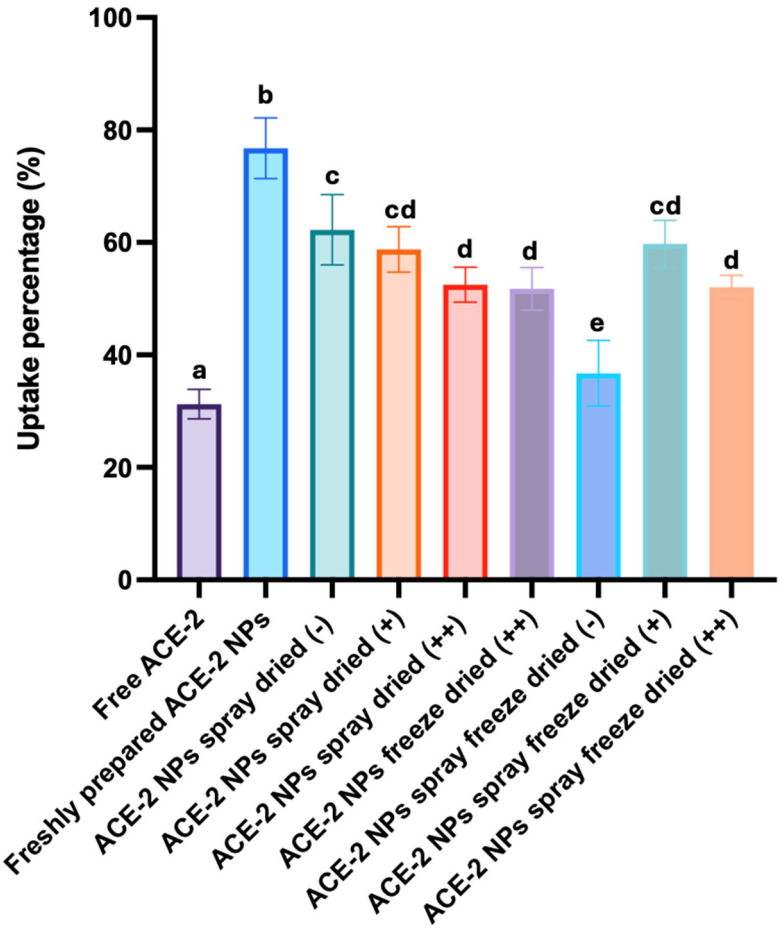

Figure 5. Caco-2 cell uptake of ACE-2, freshly prepared ACE-2 NPs, and ACE-2 NPs dehydrated in different ways. -= no mannitol; + =low mannitol; ++= high mannitol. Values represent mean + SD (n=3). Different superscripts a,b,c, in rows represent statistical difference (ANOVA; $P<0.05$).

3.7. In Vitro Toxicity Evaluation of Dehydrated ACE-2 NPs

The MTT assay was used to determine possible cytotoxicity of all dehydrated ACE-2 NPs Figure 6). Both free ACE-2 and dehydrated ACE-2 NPs showed no signs of Caco-2 reduced cell redox balance at concentrations ranging from 50 to 500 μg/mL.

 doi:10.20944/preprints202502.0602.v1

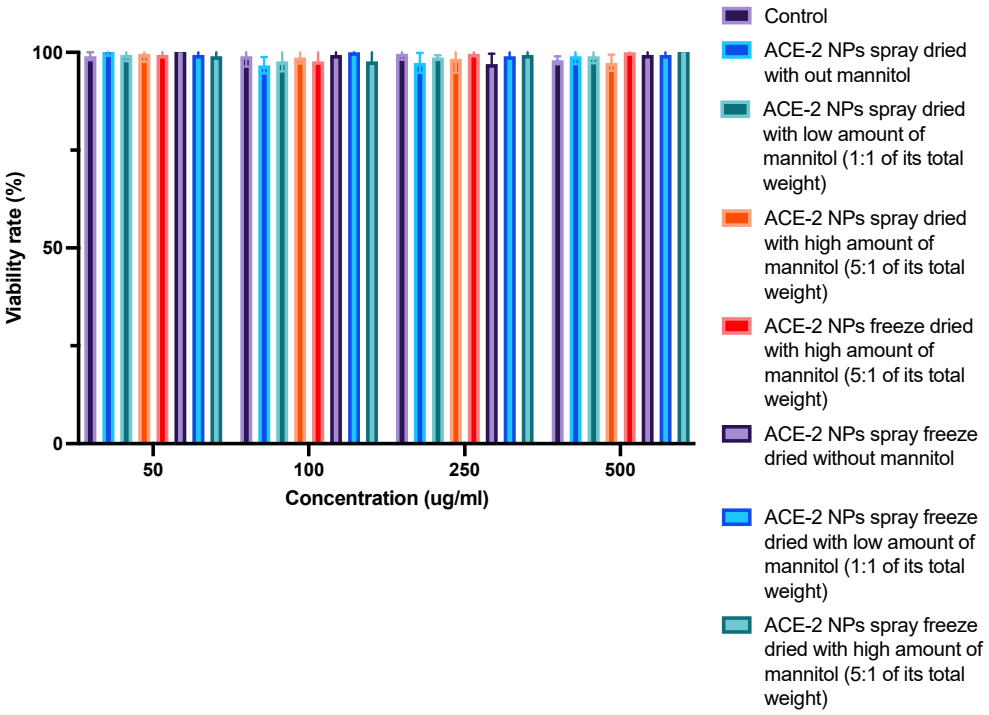

Figure 6. Caco-2 cell MTT responses to ACE-2 NPs dehydrated in different ways. Values represent mean + SD (n=3).

5. Conclusions

The present study examined the effect of varying different processing parameters (e.g., pH, mixing ratio, dehydration method, mannitol concentration) on the encapsulation efficiency and capacity of synthesized ACE-2 in chitosan/TPP constructed NPs. Employing a pH 5.5 with a chitosan: ACE-2 ratio of 2:1; produced optimal particle size of 303.7 nm, and a 98.4% EE. After dehydration, the spherical structures of ACE-2 NPs, remained intact for SFD and FD processed samples having mannitol weight ratio of 5:1. After reconstitution, however, all SD samples produced a low yield rate, especially the FD ACE-2 NPs containing high mannitol that also had the largest particle size. Only the SFD ACE-2 NPs, with low amount of mannitol (1:1 of its total weight) had both a high yield rate, similar PDI and EE, and effective particle size for ACE-2 loading. The release behavior of ACE-2 from all dehydrated NPs was rapid at both pH 2.5 and 7 solutions, while greater stability was observed at pH 6.0. The ACE-2 NPs dehydrated using SD without mannitol, and SFD using a low mannitol (1:1 of total weight) both showed a relatively fast release in media and a high Caco-2 cell uptake. However, considering the relatively low yield rate of using SD dehydration along with the high cost of ACE-2, it was concluded that the SFD process was most suitable for the production of powdered ACE-2 NPs. The findings of this research will add to the current knowledge base available for constructing non-invasive ACE-2 delivery systems to target SARS-CoV-2.

Supplementary Materials: The following supporting information can be downloaded at the website of this paper posted on Preprints.org.

Acknowledgments: The authors would like to acknowledge the following funding sources: Natural Sciences and Engineering Research Council of Canada (ALLRP 554607-2020) entitled "Encapsulation of recombinant ACE2 for the reduction of the reproduction rate of SARS-CoV-2" and the Tri-agency New Frontiers in Research Fund (NFRFR-2021-00173) entitled "In-vitro and In-vivo trials on the aerosolized rhACE2 intranasal delivery approach for treating mild COVID-19 patients".

Conflicts of Interest: The authors declare no competing interests

 doi:10.20944/preprints202502.0602.v1

References

1. Wang, Z.; Hu, S.; Popowski, K. D.; Liu, S.; Zhu, D.; Mei, X.; Li, J.; Hu, Y.; Dinh, P.-U. C.; Wang, X., Inhalation of ACE2-expressing lung exosomes provides prophylactic protection against SARS-CoV-2. *Nature Communications* **2024,** 15, (1), 2236.
2. Saito, A.; Irie, T.; Suzuki, R.; Maemura, T.; Nasser, H.; Uriu, K.; Kosugi, Y.; Shirakawa, K.; Sadamasu, K.; Kimura, I., Enhanced fusogenicity and pathogenicity of SARS-CoV-2 Delta P681R mutation. *Nature* **2022,** 602, (7896), 300-306.
3. Baldelli, A.; Wong, C. Y. J.; Oguzlu, H.; Gholizadeh, H.; Guo, Y.; Ong, H. X.; Singh, A.; Traini, D.; Pratap-Singh, A., Nasal delivery of encapsulated recombinant ACE2 as a prophylactic drug for SARS-CoV-2. *International Journal of Pharmaceutics* **2024,** 655, 124009.
4. Mannar, D.; Saville, J. W.; Zhu, X.; Srivastava, S. S.; Berezuk, A. M.; Zhou, S.; Tuttle, K. S.; Kim, A.; Li, W.; Dimitrov, D. S., Structural analysis of receptor binding domain mutations in SARS-CoV-2 variants of concern that modulate ACE2 and antibody binding. *Cell Reports* **2021,** 37, (12).
5. Zoufaly, A.; Poglitsch, M.; Aberle, J. H.; Hoepler, W.; Seitz, T.; Traugott, M.; Grieb, A.; Pawelka, E.; Laferl, H.; Wenisch, C., Human recombinant soluble ACE2 in severe COVID-19. *The Lancet Respiratory Medicine* **2020,** 8, (11), 1154-1158.
6. Diao, X.; Jia, R.; Wang, Y.; Liu, G.; Chen, X.; Liu, D.; Guan, H., The physicochemical properties, microstructure, and stability of diacylglycerol-loaded multilayer emulsion based on protein and polysaccharides. *LWT* **2024,** 196, 115879.
7. Mohammed, M. A.; Syeda, J. T.; Wasan, K. M.; Wasan, E. K., An overview of chitosan nanoparticles and its application in non-parenteral drug delivery. *Pharmaceutics* **2017,** 9, (4), 53.
8. Rampino, A.; Borgogna, M.; Blasi, P.; Bellich, B.; Cesàro, A., Chitosan nanoparticles: Preparation, size evolution and stability. *International journal of pharmaceutics* **2013,** 455, (1-2), 219-228.
9. Balde, A.; Kim, S.-K.; Benjakul, S.; Nazeer, R. A., Pulmonary drug delivery applications of natural polysaccharide polymer derived nano/micro-carrier systems: A review. *International Journal of Biological Macromolecules* **2022,** 220, 1464-1479.
10. Rezvankhah, A.; Emam-Djomeh, Z.; Askari, G., Encapsulation and delivery of bioactive compounds using spray and freeze-drying techniques: A review. *Drying Technology* **2020,** 38, (1-2), 235-258.
11. Guo, Y.; Baldelli, A.; Singh, A.; Fathordoobady, F.; Kitts, D.; Pratap-Singh, A., Production of high loading insulin nanoparticles suitable for oral delivery by spray drying and freeze drying techniques. *Scientific reports* **2022,** 12, (1), 9949.
12. Vishali, D.; Monisha, J.; Sivakamasundari, S.; Moses, J.; Anandharamakrishnan, C., Spray freeze drying: Emerging applications in drug delivery. *Journal of Controlled Release* **2019,** 300, 93-101.
13. Eggerstedt, S. N.; Dietzel, M.; Sommerfeld, M.; Süverkrüp, R.; Lamprecht, A., Protein spheres prepared by drop jet freeze drying. *International journal of pharmaceutics* **2012,** 438, (1-2), 160-166.
14. Ishwarya, S. P.; Anandharamakrishnan, C.; Stapley, A. G., Spray-freeze-drying: A novel process for the drying of foods and bioproducts. *Trends in Food Science & Technology* **2015,** 41, (2), 161-181.
15. Gan, Q.; Wang, T.; Cochrane, C.; McCarron, P., Modulation of surface charge, particle size and morphological properties of chitosan–TPP nanoparticles intended for gene delivery. *Colloids and Surfaces B: Biointerfaces* **2005,** 44, (2-3), 65-73.
16. Kumar, S.; Gokhale, R.; Burgess, D. J., Sugars as bulking agents to prevent nano-crystal aggregation during spray or freeze-drying. *International journal of pharmaceutics* **2014,** 471, (1-2), 303-311.